

Substituent Effects on Isocyanate Insertion into a Lanthanide–Sulfur Bond. Unexpected Construction of a Coordinated Thiazolate Ring

Jie Zhang,[†] Liping Ma,[†] Ruifang Cai,[†] Linhong Weng,[†] and Xigeng Zhou^{*,†,‡}

Department of Chemistry, Shanghai Key Laboratory of Molecular Catalysis and Innovative Materials, Fudan University, Shanghai 200433, People's Republic of China, and State Key Laboratory of Organometallic Chemistry, Shanghai 200032, People's Republic of China

Received September 23, 2004

[Cp₂Yb(*o*-H₂NC₆H₄S)]₂·2THF (**1**) and Cp₂Yb(*p*-H₂NC₆H₄S)(THF) (**2**) were prepared in good yields by the protonolysis of Cp₃Yb with the corresponding amino-substituted thiophenol in THF at room temperature, respectively. Treatment of [Cp₂Yb(*o*-H₂NC₆H₄S)]₂·2THF (**1**) with PhNCO gives the unexpected intermolecular addition/cyclization/elimination product [(C₅H₅)₂-Yb(μ - η^1 : η^3 -OSNC₇H₄)]₂ (**3**), while Cp₂Yb(*p*-H₂NC₆H₄S)(THF) (**2**) reacts with PhNCO under the same conditions to form the simple insertion product {Cp₂Yb[μ - η^1 : η^3 -OC(*p*-H₂NC₆H₄S)-NPh]}₂·2THF (**4**), demonstrating that the neighboring NH₂ group participation could lead to unique isocyanate insertion reactivity. The structures of all the complexes were confirmed by X-ray single-crystal diffraction analysis, indicating that complexes **1** and **4** have an unusual intermolecular hydrogen bond interaction involving THF, and a novel intramolecular π - π weak interaction between aromatic rings is also observed in **4**.

Introduction

There is currently considerable interest in studying insertions into lanthanide–ligand bonds, because they permit unusual organolanthanide derivatives to be prepared and provide new bond-forming methods for organic synthesis with exquisite selectivity and effectiveness.^{1,2} In addition, the observation and isolation of intermediate structures can provide glimpses of the mechanism of lanthanide-promoted transformation of organic functionalities.³ Although stoichiometric insertions of small molecules into lanthanide–ligand bonds have been studied extensively, surprisingly little is known about the neighboring substituent participation interaction.⁴ Furthermore, in contrast to the C–N bond-

forming reactions,^{1b,3} very few studies have emphasized the organolanthanide-promoted C–S bond formations.⁵ To the best of our knowledge, no example of organolanthanide-promoted construction of sulfur-containing heterocycles has been reported to date. Therefore, it would be of great interest to determine if individual C–S and C–N bond-forming and C–N bond-cleaving steps could be coupled using a single lanthanide center in a one-pot reaction. In this contribution, we present the first example of the further interaction of the adjacent NH₂ group with an isocyanate unit inserted into the lanthanide–sulfur bond, allowing the construction of a coordinated thiazole ring.

Results and Discussion

[Cp₂Yb(*o*-H₂NC₆H₄S)]₂·2THF (**1**) and Cp₂Yb(*p*-H₂NC₆H₄S)(THF) (**2**) were prepared by the protonolysis of Cp₃Yb with the corresponding amino-substituted thiophenol in THF at room temperature in 63 and 61% yields, respectively. It is interesting to note that the unexpected benzothiazole 2-oxide complex Cp₂Yb(μ - η^1 : η^3 -OSNC₇H₄)]₂ (**3**) was obtained as yellow crystals in 53% yield when **1** reacted with 1 equiv of PhNCO in THF at ambient temperature, indicating that the adjacent NH₂ group undergoes immediately a tandem intramolecular hydroamination/PhNH₂ elimination on insertion of PhNCO into the Yb–S bond (Scheme 1).

Although a wide variety of metal-promoted transformation reactions of isocyanates have been studied, indicating that both the C=N and the C=O double bonds of isocyanates can participate in polar addition

* To whom correspondence should be addressed at Fudan University.

[†] Fudan University.

[‡] State Key Laboratory of Organometallic Chemistry.

(1) Reviews: (a) Evans, W. J.; Davis, B. L. *Chem. Rev.* **2002**, *102*, 2119. (b) Zhou, X. G.; Zhu, M. *J. Organomet. Chem.* **2002**, *647*, 28. (c) Ferrence, G. M.; Takats, J. *J. Organomet. Chem.* **2002**, *647*, 84.

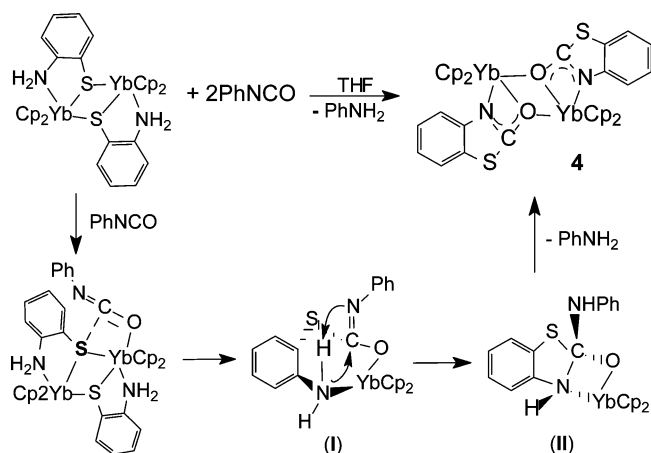
(2) (a) Kirillov, E.; Lehmann, C. W.; Razavi, A.; Carpentier, J. F. *Eur. J. Inorg. Chem.* **2004**, 943. (b) Zhang, J.; Cai, R. F.; Weng, L. H.; Zhou, X. G. *Organometallics* **2004**, *23*, 3303. (c) Beetstra, D. J.; Meetsma, A.; Hessen, B.; Teuben, J. H. *Organometallics* **2003**, *22*, 4372. (d) Voth, P.; Arndt, S.; Spaniol, T. P.; Okuda, J.; Ackerman, L. J.; Green, M. L. H. *Organometallics* **2003**, *22*, 65. (e) Kornienko, A. Y.; Emge, T. J.; Brennan, J. G. *J. Am. Chem. Soc.* **2001**, *123*, 11933. (f) Evans, W. J.; Fujimoto, C. H.; Ziller, J. W. *Organometallics* **2001**, *20*, 4529. (g) Evans, W. J.; Kozimor, S. A.; Nyce, G. W.; Ziller, J. W. *J. Am. Chem. Soc.* **2003**, *125*, 13831. (h) Zhang, J.; Cai, R. F.; Weng, L. H.; Zhou, X. G. *Organometallics* **2003**, *22*, 5385.

(3) (a) Molander, G. A.; Romero, J. A. C. *Chem. Rev.* **2002**, *102*, 2161 and references therein. (b) Hong, S. W.; Kawaoka, A. M.; Marks, T. J. *J. Am. Chem. Soc.* **2003**, *125*, 15878. (c) Hong, S. W.; Tian, S.; Metz, M. V.; Marks, T. J. *J. Am. Chem. Soc.* **2003**, *125*, 14768. (d) Molander, G. A.; Pack, S. K. *J. Org. Chem.* **2003**, *68*, 9214. (e) Gribkov, D. V.; Hultsch, K. C.; Hampel, F. *Chem. Eur. J.* **2003**, *9*, 4796. (f) Hultsch, K. C.; Hampel, F.; Wagner, T. *Organometallics* **2004**, *23*, 2601. (g) Hong, S.; Marks, T. J. *Acc. Chem. Res.* **2004**, *37*, 673.

(4) Evans, W. J.; Hughes, L. A.; Drummond, D. K.; Zhang, H.; Atwood, J. L. *J. Am. Chem. Soc.* **1986**, *108*, 1722.

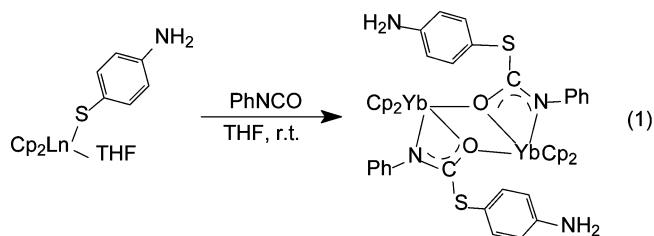
(5) (a) Shen, Q.; Li, H. R.; Yao, C. S.; Yao, Y. M.; Zhang, L. L.; Yu, K. B. *Organometallics* **2001**, *20*, 3070. (b) Zhang, C. M.; Liu, R. T.; Zhou, X. G.; Chen, Z. X.; Weng, L. H.; Lin, Y. H. *Organometallics* **2004**, *23*, 3246.

Scheme 1



reactions, in most cases only single-addition products are isolated, and the sequential C=O and C=N bis-addition processes are rarely observed.^{1,6} To our knowledge, only one stepwise addition reaction of organometallic reagents to isocyanates has been reported, where the isocyanate unit inserted into the Zr–H bond, forming a formamido ligand, with further addition of a second Zr–H bond.⁷ The further addition reaction of an organic functionality to the isocyanate unit inserted into the metal–ligand bond is unprecedented. On the other hand, organolanthanides have been applied successfully to the intra-/intermolecular hydroamination and hydrophosphination of a variety of unsaturated substrates, including aminoolefins, aminoalkynes, phosphinoalkenes, and phosphinoalkynes, providing a mild and efficient method for the construction of aza- and phosphacyclic skeletons.^{3,8} To our knowledge, the present regioselective, tandem C–S and C–N bond-forming and subsequent C–N bond-cleaving reaction is unprecedented in organolanthanide chemistry and provides an effective method for the construction of the thiazole skeleton, despite the fact that it is stoichiometric with respect to the metal fragment.

To obtain additional insight into the mechanism and scope of the reaction, we examined the behavior of Cp₂Yb(*p*-H₂NC₆H₄S)(THF) (**2**) toward PhNCO. In marked contrast to [Cp₂Yb(*o*-H₂NC₆H₄S)]₂·2THF, where multiple pathways occur for PhNCO, treatment of **2** with 1 equiv of PhNCO under the same conditions provided only the dinuclear insertion product {Cp₂Yb[μ-η¹:η³-OC(*p*-H₂NC₆H₄S)NPh]}₂·2THF (**4**) (eq 1). The direct



addition of amines to isocyanates is a convenient transformation in organic synthesis.⁹ However, this result indicates that PhNCO is preferentially added by

the Yb–S bond rather than the N–H bond. The free NH₂ group at the para position is inert and undergoes neither competitive addition to PhNCO nor further addition to the newly formed OC(*p*-H₂NC₆H₄S)NPh ligand under the conditions involved. Recently, lanthanide thiolates were found to have high catalytic activities for oligomerization of phenyl isocyanate,¹⁰ but no oligomerization of phenyl isocyanate occurred and only insertion chemistry is observed in the treatment of PhNCO with **1** and **2**.

On the basis of these experimental results, a possible reaction pathway for the formation of **3** is proposed in Scheme 1. Coordination of PhNCO and migration of *o*-H₂NC₆H₄S give the insertion intermediate **I**. A sequential addition of the activated N–H to the C=N double bond results in cyclization via a four-centered σ bond metathesis process. Reductive elimination of PhNH₂ generates the thiazolate ring. Obviously, the present hydroamination/cyclization pathway is different from the mechanism of the previously reported organolanthanide-catalyzed construction of azacyclic skeletons: for the latter the hydroamination/cyclization reaction generally proceeds via a turnover-limiting C–C multiple-bond insertion into the lanthanide–nitrogen bond.^{3g} However, attempts to isolate the intermediate **II** have been unsuccessful, due to the thermodynamic instability. A tandem addition/cyclization/elimination reaction is observed in the treatment of **1** with PhNCO, whereas for **2** no subsequent reaction is observed, even with a longer reaction time. It is possible that both the activation of the metal on the NH₂ group and the formation of a more stable aromatic thiazolate skeleton contribute to the occurrence of the hydroamination/cyclization/amine-elimination reaction of the putative amido intermediate **I**. Furthermore, this reaction also represents the first example in organolanthanide chemistry of direct N–H addition to a ligand functionality.

Complexes **1**–**4** have been characterized by elemental analysis and IR and mass spectroscopy, which were in good agreement with the proposed structures. Interestingly, in the IR spectra compound **2** displays three medium-intensity bands at 3554, 3409, and 3318 cm⁻¹ attributable to ν(N–H) vibrations, while the corresponding bands due to the H-bond interaction in **4** are observed near 3430, 3343, and 3230 cm⁻¹, respectively. In the case of **1** the absorptions of N–H bonds are shifted to lower frequencies with a medium band at 3238 cm⁻¹ and a weaker band at 3170 cm⁻¹ as compared with **4**, which may be attributed to the additional chelating coordination as established by X-ray diffraction. The structures of all the complexes were also confirmed by X-ray single-crystal diffraction analysis. Crystal structure analysis confirmed that complex **1** is a centrosymmetric dimeric structure, with the *o*-aminothiophenoxyl ligand as both a bridging and side-on donating group. Each Yb atom is coordinated by two cyclopentadienyl rings, two bridging sulfur atoms, and one chelating nitrogen atom to form an edge-bridged tetrahedral geometry. The Yb–N distance (2.459(2) Å; Table 2) is

(8) (a) Douglass, M. R.; Stern, C. L.; Marks, T. J. *J. Am. Chem. Soc.* **2001**, *123*, 10221. (b) Kawaoka, A. M.; Douglass, M. R.; Marks, T. J. *Organometallics* **2003**, *22*, 4630.

(9) Ozaki, S. *Chem. Rev.* **1972**, *72*, 457.

(10) Deng, M. Y.; Yao, Y. M.; Zhou, Y. F.; Zhang, L. F.; Shen, Q. *Chin. J. Chem.* **2003**, *21*, 574.

(6) Braunstein, P.; Nobel, D. *Chem. Rev.* **1989**, *89*, 1927.

(7) Gambarotta, S.; Strologo, S.; Floriani, C.; Chiesi-Villa, A.; Guastini, C. *J. Am. Chem. Soc.* **1985**, *107*, 6278.

Table 1. Crystal and Data Collection Parameters of Complexes 1–4

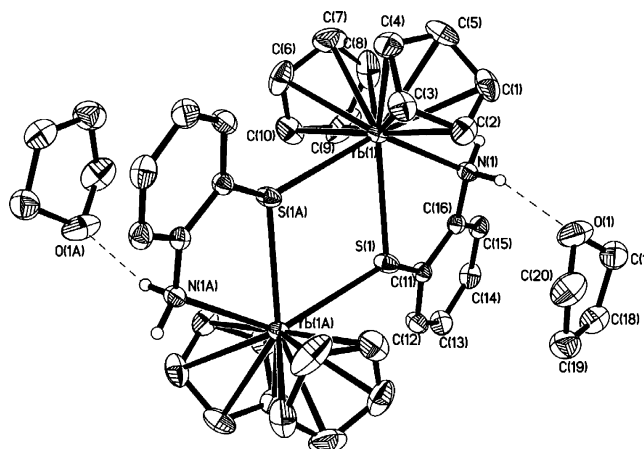
	1	2	3	4
formula	C ₄₀ H ₄₈ N ₂ O ₂ S ₂ Yb ₂	C ₂₀ H ₂₄ NOSYb	C ₄₂ H ₄₄ N ₂ O ₄ S ₂ Yb ₂	C ₅₄ H ₅₀ N ₄ O ₄ S ₂ Yb ₂
mol wt	999.00	499.50	1050.99	1237.24
cryst color	red	orange	orange	orange
cryst dimens (mm)	0.35 × 0.25 × 0.20	0.10 × 0.08 × 0.05	0.25 × 0.10 × 0.08	0.35 × 0.20 × 0.10
cryst syst	monoclinic	triclinic	monoclinic	triclinic
space group	<i>P</i> 2 ₁ / <i>c</i>	<i>P</i> 1	<i>P</i> 2 ₁ / <i>n</i>	<i>P</i> 1
unit cell dimens				
<i>a</i> (Å)	10.9171(12)	7.768(2)	14.052(4)	11.112(6)
<i>b</i> (Å)	10.6077(12)	8.653(3)	8.375(3)	11.338(6)
<i>c</i> (Å)	16.9229(18)	14.462(4)	17.511(5)	12.039(6)
α (deg)		84.112(4)		115.778(5)
β (deg)	103.9650(10)	83.848(4)	105.223(4)	101.400(7)
γ (deg)	1901.8(4)	89.238(4)	1988.6(11)	100.963(7)
<i>V</i> (Å ³)		961.4(5)		1271.7(11)
<i>Z</i>	2	2	2	1
<i>D</i> _c (g cm ⁻³)	1.745	1.726	1.755	1.615
μ (mm ⁻¹)	5.033	4.978	4.822	3.785
<i>F</i> (000)	980	490	1028	614
radiation ($\lambda = 0.710 730$ Å)			Mo K α	
temp (K)	293.2	298.2	298.2	298.2
scan type			$\omega-2\theta$	
θ range (deg)	2.29–26.51	1.42–26.01	1.66–25.01	1.97–25.01
<i>h, k, l</i> range	–13 ≤ <i>h</i> ≤ 11 –12 ≤ <i>k</i> ≤ 13 –20 ≤ <i>l</i> ≤ 21	–8 ≤ <i>h</i> ≤ 9 –10 ≤ <i>k</i> ≤ 8 –17 ≤ <i>l</i> ≤ 17	–15 ≤ <i>h</i> ≤ 16 –8 ≤ <i>k</i> ≤ 9 –20 ≤ <i>l</i> ≤ 20	–6 ≤ <i>h</i> ≤ 13 –13 ≤ <i>k</i> ≤ 12 –12 ≤ <i>l</i> ≤ 13
no. of rflns measd	8904	4432	7971	4617
no. of unique rflns	3921 (<i>R</i> _{int} = 0.0204)	3709 (<i>R</i> _{int} = 0.0201)	3481 (<i>R</i> _{int} = 0.0383)	4166 (<i>R</i> _{int} = 0.0290)
completeness to θ (%)	99.5 ($\theta = 26.51^\circ$)	97.6 ($\theta = 26.01^\circ$)	99.8 ($\theta = 25.01^\circ$)	92.8 ($\theta = 25.01^\circ$)
max and min transmissn	0.4326 and 0.2718	0.7889 and 0.6359	0.6990 and 0.3786	0.7034 and 0.3509
refinement method		full-matrix least squares on <i>F</i> ²		
no. of data/restraints/params	3921/0/218	3709/0/217	3481/0/210	4166/0/273
goodness of fit on <i>F</i> ²	0.989	0.988	0.947	1.081
final <i>R</i> indices (<i>I</i> > 2 σ (<i>I</i>))	<i>R</i> 1 = 0.0189, w <i>R</i> 2 = 0.0435	<i>R</i> 1 = 0.0338, w <i>R</i> 2 = 0.779	<i>R</i> 1 = 0.0440, w <i>R</i> 2 = 0.1156	<i>R</i> 1 = 0.0457, w <i>R</i> 2 = 0.1287
<i>R</i> indices (all data)	<i>R</i> 1 = 0.0236, w <i>R</i> 2 = 0.0445	<i>R</i> 1 = 0.410, w <i>R</i> 2 = 0.796	<i>R</i> 1 = 0.0676, w <i>R</i> 2 = 0.1214	<i>R</i> 1 = 0.0505, w <i>R</i> 2 = 0.1353
largest diff peak and hole (e Å ⁻³)	0.667 and –0.609	1.347 and –1.008	0.937 and –0.950	1.749 and –1.430

Table 2. Selected Bond Lengths (Å) and Angles (deg) for Complex 1

Yb(1)–N(1)	2.459(2)	Yb(1)–C(2)	2.654(3)
Yb(1)–C(8)	2.590(4)	Yb(1)–C(1)	2.669(3)
Yb(1)–C(4)	2.599(3)	Yb(1)–S(1)	2.724(1)
Yb(1)–C(10)	2.602(3)	S(1)–C(11)	1.762(3)
Yb(1)–C(9)	2.606(4)	S(1)–Yb(1A)	2.864(1)
Yb(1)–C(6)	2.606(3)	N(1)–C(16)	1.442(3)
Yb(1)–C(7)	2.608(4)	N(1)···O(1)	2.992(4)
Yb(1)–C(5)	2.624(3)	O(1)···H(1B)	2.13
Yb(1)–C(3)	2.626(3)		
N(1)–Yb(1)–S(1)	67.4(1)	C(16)–N(1)–Yb(1)	117.0(2)
C(11)–S(1)–Yb(1)	101.6(1)	C(16)–C(11)–S(1)	117.3(2)
C(11)–S(1)–Yb(1A)	131.6(1)	C(11)–C(16)–N(1)	117.2(2)
Yb(1)–S(1)–Yb(1A)	113.4(1)	N(1)–H(1B)···O(1)	159.9

comparable with the Yb–N donor bond distance of Cp₂Yb[OC(=NPh)PzMe₂](THF) (2.473(2) Å).^{2h} An interesting feature of the crystal structure of **1** is the N(1)–H(1B)···O(1) hydrogen bonding between the chelating coordinated NH₂ group and the uncoordinated THF, as shown in Figure 1. The hydrogen-bond interaction is common in inorganic complexes of rare earths.¹¹ For the lanthanocene system, however, a similar interaction is quite uncommon¹² and no example of a hydrogen-bond interaction involving THF has been reported.

Complex **2** is a solvated monomeric structure (Figure 2) and has normal metrical parameters (Table 3). The Yb–S distance of 2.641(2) Å is shorter than the Yb–S

**Figure 1.** ORTEP diagram of [Cp₂Yb(*o*-H₂NC₆H₄S)]₂·2THF (**1**) with the ellipsoids drawn at the 30% probability level.

distances in **1**, in which the sulfur atoms are in bridging positions. This shortening of 0.083–0.223 Å is quite normal on going from bridging to nonbridging and is in the range observed for organolanthanide chloride complexes (0.04–0.27 Å).¹³

The molecular structure of **3** is shown in Figure 3. Selected bond lengths and angles of **3** are listed in Table 4. The X-ray crystal analysis results show that the benzothiazole 2-oxide ligand in **3** exhibits an unusual

(11) Liang, Y. C.; Cao, R.; Su, W. P.; Hong, M. C.; Zhang, W. J. *Angew. Chem., Int. Ed.* **2000**, *39*, 3304.

(12) Shapiro, P. L.; Henling, L. M.; Marsh, R. E.; Bercaw, J. E. *Inorg. Chem.* **1990**, *29*, 4560.

(13) Evans, W. J.; Peterson, T. T.; Rausch, M. D.; Hunter, W. J.; Atwood, J. L. *Organometallics* **1985**, *4*, 554.

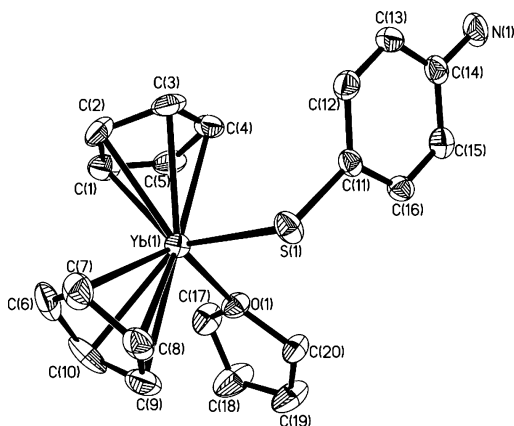


Figure 2. ORTEP diagram of $\text{Cp}_2\text{Yb}(p\text{-H}_2\text{NC}_6\text{H}_4\text{S})(\text{THF})$ (**2**) with the ellipsoids drawn at the 30% probability level.

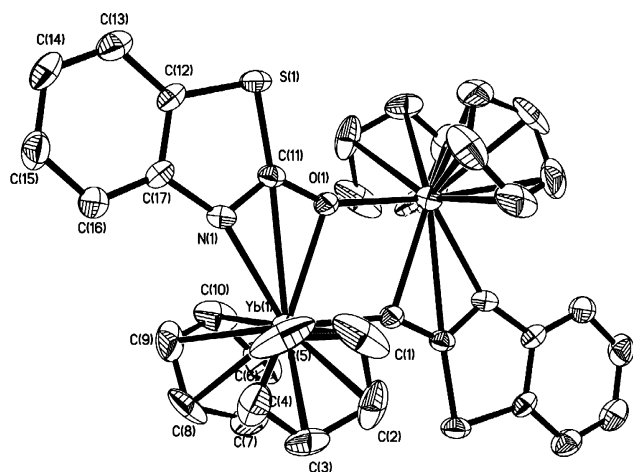


Figure 3. ORTEP diagram of $[\text{Cp}_2\text{Yb}(o\text{-H}_2\text{NC}_6\text{H}_4\text{S})]_2$ (**3**) with the ellipsoids drawn at the 30% probability level.

Table 3. Selected Bond Lengths (Å) and Angles (deg) for Complex 2

Yb(1)–O(1)	2.287(4)	Yb(1)–C(10)	2.614(7)
Yb(1)–C(7)	2.583(6)	Yb(1)–C(4)	2.620(6)
Yb(1)–C(2)	2.584(6)	Yb(1)–C(9)	2.625(7)
Yb(1)–C(6)	2.589(7)	Yb(1)–S(1)	2.641(2)
Yb(1)–C(1)	2.594(6)	Yb(1)–C(5)	2.645(6)
Yb(1)–C(3)	2.597(6)	S(1)–C(11)	1.786(6)
Yb(1)–C(8)	2.610(6)		
O(1)–Yb(1)–S(1)	99.4(1)	C(11)–S(1)–Yb(1)	106.7(2)

bonding mode, which acts as both a bridging and side-on chelating group. Both the O(1)–C(11) and N(1)–C(11) distances of 1.264(10) and 1.286(10) Å lie between single- and double-bond distances.¹⁴ This suggests some electronic delocalization over the O–C–N unit. Consistent with this, the Yb(1)–N(1) distance of 2.461(6) Å is between those expected for a $\text{Yb}^{3+}\text{--N}$ single bond and a $\text{Yb}^{3+}\text{--}\leftarrow\text{N}$ donor bond (2.19–2.69 Å),¹⁵ and there is a weak interaction between Yb(1) and C(11).

Complex **4** is a dimeric structure (Figure 4). The structural data reveal that PhNCO has inserted into the Yb–S bond to form a thiolate-substituted amido anion. Characteristically, the unusual intermolecular hydrogen-bond interaction between the noncoordinated

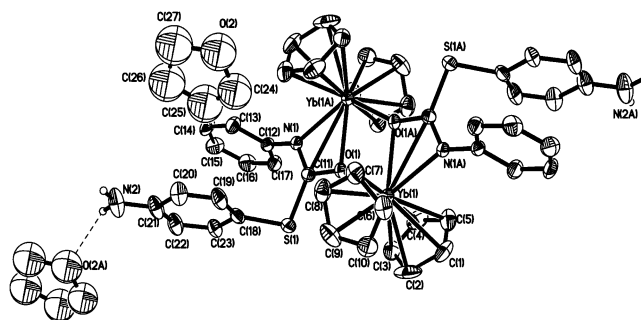


Figure 4. ORTEP diagram of $\{\text{Cp}_2\text{Yb}[\mu\text{-}\eta^1:\eta^3\text{-OC}(p\text{-H}_2\text{NC}_6\text{H}_4\text{S})\text{NPh}]\}_2\cdot 2\text{THF}$ (**4**) with the ellipsoids drawn at the 30% probability level.

Table 4. Selected Bond Lengths (Å) and Angles (deg) for Complex 3

Yb(1)–O(1A)	2.288(6)	Yb(1)–C(5)	2.601(12)
Yb(1)–O(1)	2.414(7)	Yb(1)–C(4)	2.602(11)
Yb(1)–N(1)	2.461(6)	Yb(1)–C(1)	2.604(12)
Yb(1)–C(8)	2.583(10)	S(1)–C(12)	1.741(9)
Yb(1)–C(9)	2.590(11)	S(1)–C(11)	1.764(8)
Yb(1)–C(3)	2.593(10)	O(1)–C(11)	1.264(10)
Yb(1)–C(7)	2.593(10)	N(1)–C(11)	1.286(10)
Yb(1)–C(6)	2.595(11)	N(1)–C(17)	1.434(10)
Yb(1)–C(10)	2.598(11)		
O(1A)–Yb(1)–N(1)	119.4(2)	C(17)–N(1)–Yb(1)	154.2(6)
O(1A)–Yb(1)–O(1)	65.5(2)	O(1)–C(11)–N(1)	120.2(7)
N(1)–Yb(1)–O(1)	53.9(2)	O(1)–C(11)–S(1)	124.3(7)
C(12)–S(1)–C(11)	88.7(4)	N(1)–C(11)–S(1)	115.4(7)
C(11)–O(1)–Yb(1)	92.1(5)	O(1)–C(11)–Yb(1)	61.1(4)
Yb(1A)–O(1)–Yb(1)	114.5(2)	N(1)–C(11)–Yb(1)	59.1(4)
C(11)–N(1)–C(17)	112.1(7)	S(1)–C(11)–Yb(1)	174.3(5)
C(11)–N(1)–Yb(1)	93.7(5)		

Table 5. Selected Bond Lengths (Å) and Angles (deg) for 4

Yb(1)–O(1)	2.268(5)	Yb(1)–C(7)	2.621(8)
Yb(1)–O(1A)	2.372(5)	S(1)–C(18)	1.774(9)
Yb(1)–N(1A)	2.414(5)	S(1)–C(11)	1.778(7)
Yb(1)–C(9)	2.583(9)	N(1)–C(11)	1.262(9)
Yb(1)–C(1)	2.583(9)	N(1)–C(12)	1.415(9)
Yb(1)–C(5)	2.594(9)	N(1)–Yb(1A)	2.414(5)
Yb(1)–C(2)	2.603(9)	O(1)–C(11)	1.309(8)
Yb(1)–C(3)	2.614(8)	O(1)–Yb(1A)	2.372(5)
Yb(1)–C(4)	2.616(9)	N(2)···O(2A)	3.10(2)
Yb(1)–C(10)	2.622(9)	O(2)···H(2A)	2.38
Yb(1)–C(8)	2.617(9)		
O(1)–Yb(1)–O(1A)	66.0(2)	Yb(1)–O(1)–Yb(1A)	114.0(2)
O(1)–Yb(1)–N(1A)	120.2(2)	N(1)–C(11)–O(1)	116.4(6)
O(1A)–Yb(1)–N(1A)	54.3(2)	N(1)–C(11)–S(1)	128.8(5)
C(18)–S(1)–C(11)	102.6(4)	O(1)–C(11)–S(1)	114.7(5)
C(11)–N(1)–C(12)	123.2(6)	N(1)–C(11)–Yb(1A)	59.1(4)
C(11)–N(1)–Yb(1A)	94.2(4)	O(1)–C(11)–Yb(1A)	57.4(3)
C(12)–N(1)–Yb(1A)	141.6(5)	S(1)–C(11)–Yb(1A)	172.1(4)
C(11)–O(1)–Yb(1)	150.6(5)	N(2)–H(2A)···O(2A)	141.5
C(11)–O(1)–Yb(1A)	94.9(4)		

NH_2 and noncoordinated THF molecules is also observed in **4**. Bond lengths and angles involving the amido functions indicate their bonding in an $\mu\text{-}\eta^1:\eta^3$ fashion. The Yb(1)–O(1), Yb(1)–O(1A), Yb(1)–N(1A), and Yb(1)–C(11A) distances of 2.268(5), 2.372(5), 2.414(5), and 2.806(7) Å (Table 5) are similar to the corresponding distances of 2.288(6), 2.461(6), 2.414(7), and 2.808(5) Å in **3**, respectively. The distance between the centers of two aromatic rings containing C(12) and C(18) is 3.775 Å, and the dihedral angle between the least-squares planes amounts to 17.9°. These data demonstrate that the two aromatic rings are close together so that intramolecular $\pi\text{-}\pi$ interactions are

(14) Allen, F. H.; Kennard, O.; Watson, D. G.; Brammer, L.; Orpen, A. G. *J. Chem. Soc., Perkin Trans.* **1987**, S1.

(15) Zhou, X. G.; Zhang, L. B.; Zhu, M.; Cai, R. F.; Weng, L. H. *Organometallics* **2001**, *20*, 5700.

possible.¹⁶ Similar π - π stacking interactions were observed for lanthanide complexes with the doubly deprotonated form of the bibracchial lariat ether N,N' -bis(2-salicylaldiminobenzyl)-1,10-diaza-15-crown-5.¹⁷

In conclusion, the present work demonstrates the novel reactivity of organolanthanides with bifunctional ligands toward PhNCO. It is interesting to note that the further interaction of the neighboring NH_2 group with an isocyanate unit inserted into the lanthanide-sulfur bond could lead to unique reactivity and selectivity trends, allowing a mild and efficient construction of the coordinated benzothiazole 2-oxide ligand. In contrast to the known organolanthanide-promoted hydroamination/cyclization reactions, where the general mechanism involves turnover-limiting C-C multiple-bond insertion into the lanthanide-heteroatom bond followed by a rapid protonolysis by other amine substrates,^{3,8} in the present case, the hydroamination/cyclization proceeds via intramolecular amine addition to the C=N double bond. Moreover, the X-ray crystal structure analyses have revealed an unusual intermolecular hydrogen-bond interaction involving THF and an interesting intramolecular π - π weak interaction between aromatic rings.

Experimental Section

All operations involving air- and moisture-sensitive compounds were carried out under an inert atmosphere of purified nitrogen using standard Schlenk techniques. All solvents were refluxed and distilled over sodium benzophenone ketyl under nitrogen immediately prior to use. Elemental analyses for C, H, and N were carried out on a Vario EL CHN-O analyzer. Infrared spectra were obtained on a Nicolet FT-IR 360 spectrometer with samples prepared as Nujol mulls. Mass spectra were recorded on a Philips Agilent MS5973N or Philips HP5989A instrument operating in EI mode. Crystalline samples of the respective complexes were rapidly introduced by direct-inlet techniques.

Synthesis of $[\text{Cp}_2\text{Yb}(o\text{-H}_2\text{NC}_6\text{H}_4\text{S})]_2 \cdot 2\text{THF}$ (1). (C_5H_5)₃-Yb (0.968 g, 2.63 mmol) and *o*-aminothiophenol (0.329 g, 2.63 mmol) were mixed in 100 mL of THF. The solution color slowly turned from dark green to red in several hours. After the mixture was stirred for 24 h at room temperature, all volatile substances were removed under vacuum to give an orange powder. Orange crystals of **1**·2THF were obtained by recrystallization from THF at -20°C for several days. Yield: 0.768 g (63%). Anal. Calcd for $\text{C}_{40}\text{H}_{48}\text{O}_2\text{N}_2\text{S}_2\text{Yb}_2$: C, 48.09; H, 4.84; N, 2.80. Found: C, 47.93; H, 4.79; N, 2.97. IR (Nujol): 3238 m, 3170 w, 1657 m, 1587 m, 1565 m, 1061 s, 1013 s, 910 m, 770 s, 681 m cm^{-1} . EI-MS (m/z (%)): 428 (52) [M/2].

Synthesis of $\text{Cp}_2\text{Yb}(p\text{-H}_2\text{NC}_6\text{H}_4\text{S})(\text{THF})$ (2). Following the procedure described for **1**, reaction of (C_5H_5)₃Yb (0.888 g,

2.41 mmol) with *p*-aminothiophenol (0.302 g, 2.41 mmol) gave **2** as orange crystals. Yield: 0.734 g (61%). Anal. Calcd for $\text{C}_{20}\text{H}_{24}\text{NOSYb}$: C, 48.09; H, 4.84; N, 2.80. Found: C, 48.16; H, 4.92; N, 2.91. IR (Nujol): 3554 m, 3409 m, 3318 m, 1619 s, 1599 s, 1074 s, 1008 s, 911 m, 775 s, 664 m cm^{-1} . EI-MS (m/z (%)): 428 (15) [M - THF].

Reaction of Complex 1 with PhNCO. To a 30 mL THF solution of **1** (0.524 g, 0.57 mmol) was slowly added phenyl isocyanate (0.135 g, 1.14 mmol) at room temperature and stirred for 24 h. The reaction solution was concentrated to ca. 3 mL by reduced pressure. Yellow crystals of $[(\text{C}_5\text{H}_5)_2\text{Yb}(\mu\text{-}\eta^1\text{-}\eta^3\text{-OSNC}_7\text{H}_4)]_2$ (**3**) were obtained at -20°C for several days. Yield: 0.318 g (53%). Anal. Calcd for $\text{C}_{42}\text{H}_{44}\text{N}_2\text{O}_4\text{S}_2\text{Yb}_2$: C, 48.00; H, 4.22; N, 2.67. Found: C, 47.83; H, 4.11; N, 2.85. IR (Nujol): 3161 m, 1613 s, 1589 s, 1538 m, 1565 m, 1074 s, 1009 s, 920 m, 770 s, 735 s, 670 m, 657 m cm^{-1} . EI-MS (m/z (%)): 454 (25) [M/2]. The PhNH_2 produced was identified by GC/MS.

Reaction of Complex 2 with PhNCO. By the above procedure described for **3**, reaction of **2** (0.460 g, 0.92 mmol) with phenyl isocyanate (0.109 g, 0.92 mmol) gave $\{\text{Cp}_2\text{Yb}[\mu\text{-}\eta^1\text{-}\eta^3\text{-OC}(p\text{-H}_2\text{NC}_6\text{H}_4\text{S})\text{NPh}]\}_2 \cdot 2\text{THF}$ (**4**) as orange crystals. Yield: 0.262 g (46%). Anal. Calcd for $\text{C}_{54}\text{H}_{58}\text{N}_4\text{O}_4\text{S}_2\text{Yb}_2$: C, 52.42; H, 4.73; N, 4.52. Found: C, 52.39; H, 4.71; N, 4.59. IR (Nujol): 3437 m, 3343 m, 3222 m, 1634 s, 1593 s, 1550 s, 1062 s, 1010 s, 928 s, 773 s, 710 m, 695 m, 658 m cm^{-1} . EI-MS (m/z (%)) 547 (12) [M/2].

X-ray Data Collection, Structure Determination, and Refinement for 1-4. A suitable crystal for each of the complexes was selected and sealed under argon in a Lindemann glass capillary for X-ray structural analysis. Diffraction data were collected on a Bruker SMART CCD diffractometer using graphite-monochromated Mo $\text{K}\alpha$ ($\lambda = 0.71073 \text{ \AA}$) radiation. The intensities were corrected for Lorentz-polarization effects and empirical absorption with the SADABS program.¹⁸ A summary of the crystallographic data is given in Table 1.

The structure was solved by direct methods using the SHELXL-97 program.¹⁹ All non-hydrogen atoms were found from the difference Fourier syntheses. H atoms were included in calculated positions with isotropic thermal parameters related to those of the supporting carbon atoms but were not included in the refinement. There is one solvent molecule present per formula unit for **3**. All calculations were performed using the Bruker Smart program.

Acknowledgment. We thank the NNSF of China, the NSF of Shanghai, the Fund of the New Century Distinguished Scientist of the Education Ministry of China, and the Research Fund for the Doctoral Program of Higher Education of China for financial support.

Supporting Information Available: Figures giving additional views and CIF files giving details of crystal structure determinations and structure data for all complexes. This material is available free of charge via the Internet at <http://pubs.acs.org>.

OM0492606

(16) (a) Hobza, P.; Selzle, H. L.; Schlag, E. W. *J. Am. Chem. Soc.* **1994**, *116*, 3500. (b) Zhang, X.-X.; Boedunov, A. V.; Bradshaw, J. S.; Dalley, N. K.; Kou, X.; Izatt, R. M. *J. Am. Chem. Soc.* **1995**, *117*, 11507. (c) Ranganathan, D.; Haridas, V.; Gilardi, R.; Karle, I. L. *J. Am. Chem. Soc.* **1998**, *120*, 10793.

(17) González-Lorenzo, M.; Platas-Iglesias, C.; Avecilla, F.; Galdes, C. F. G. C.; Imbert, D.; Bünzli, J.-C. G.; de Blas, A.; Rodríguez-Blas, T. *Inorg. Chem.* **2003**, *42*, 6946.

(18) Sheldrick, G. M. SADABS, A Program for Empirical Absorption Correction; University of Göttingen, Göttingen, Germany, 1998.

(19) Sheldrick, G. M. SHELXL-97, Program for the Refinement of the Crystal Structure; University of Göttingen, Göttingen, Germany, 1997.